Terahertz VRT Spectroscopy of the Water Hexamer-d_{12} Prism: Dramatic enhancement of bifurcation tunneling upon librational excitation

William T. S. Cole[1], Akber A. Sheikh[1], Ozlem Yonder[1,2], Raymond S. Fellers[1,a], Mark R. Viant[1,b], Richard J. Saykally[1c]

James D. Farrell[3], David J. Wales[3]

1) Department of Chemistry, University of California, Berkeley, California 94720, USA
2) Temp
3) Department of Chemistry, University of Cambridge, Cambridge CB2 1EW, UK

a) Present Address: Picarro, 3105 Patrick Henry Drive, Santa Clara, California 95054, USA
b) Present Address: School of Biosciences, University of Birmingham, Edgbaston, Birmingham, UK B15 2TT
c) Author to whom correspondence should be addressed. Electronic mail: saykally@berkeley.edu

Keywords: Water cluster, hydrogen bond, tunneling, libration

Abstract

Introduction

The challenge with a molecular-scale description of the structure of water is partially a consequence of the extended and dynamic hydrogen-bonded network within water[1-5]. Studying water clusters provides a means of studying these clusters isolated from the bulk. The hexamer is of particular interest, as it is the smallest cluster that has a 3D, non-cyclic structure reminiscent of the three-dimensional hydrogen bond network that exists in bulk phases [4, 6-9]. Previous works have provided evidence for the existence of cage, prism, and book isomers within a supersonic expansion [8, 10-12]. It has been established that the cage isomeric structure is the global minimum energy structure, through the prism lies in close energetic proximity as evidenced by work showing the coexistence of prism and cage structures in the microwave region [4, 11, 13-17].

One of the first experimental study of a pure water hexamer cluster was reported by Liu et al and observed the cage isomer in a supersonic expansion [8, 10]. Liu showed the tunneling dynamics of the cluster bore resemblance to smaller cluster studied and establish the first structural characterization of the cage isomer. More recently, Perez et al observed the cage, prism, and book isomer (in addition to heptamer and nonamer clusters) in a supersonic expansion studied with broadband microwave spectroscopy [11, 18]. This study characterized the structures of these isomers at high resolution and provided critical insight into the associated tunneling motions. Specifically a follow-up study by Richardson et al provided an in-depth overview of the tunneling motions of the water hexamer prism, and importantly showed that the prism possesses a tunneling pathway, which simultaneously breaks two hydrogen bonds [12]. The structure and energy level diagram of the water prism is shown in Figure 1.

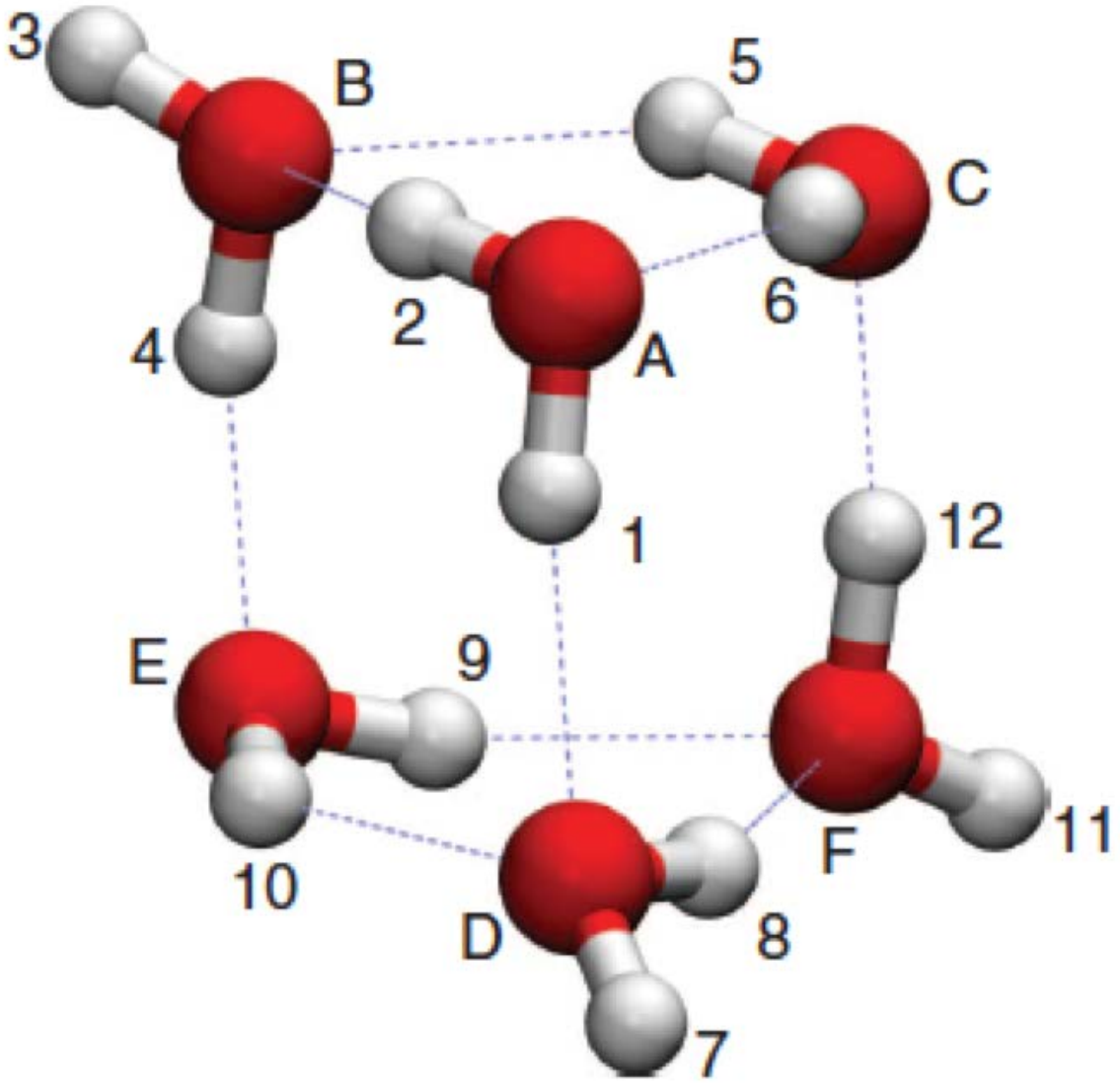

Figure 1: The lowest energy structure of the water hexamer prism, oxygens are labeled by A – F and hydrogens are labeled 1 – 12. This figure is reproduced with permission from reference 12.

There will be a paragraph here to describe the theoretical front

We have measured a parallel vibration-rotation-tunneling (VRT) hybrid band of a $(D_2O)_6$ cluster centered in the 510 cm^{-1} region. The experimental rotational constants, which measure the mass distribution in the cluster through the principal moments of inertia, extracted from the present VRT spectra agree most closely with those predicted for the prism structure. We saw an enhancement in the bifurcation tunneling of the D_2O cluster relative to the ground state, in keeping with other studies in this region [19-22]. To our knowledge this is the first high-resolution study of a D_2O hexamer cluster in the terahertz region.

Experimental

Our previous investigations of water dimer, trimer, and pentamer librational motion in the 500 cm^{-1} region prompted us to search for transitions from larger clusters [22, 23]. The Berkeley diode laser/supersonic beam spectrometer used in this study has been described in detail elsewhere and only a short description is provided here [24, 25].

A helium-cooled spectrometer (Spectra Physics) using lead-salt diodes (Laser Photonics) was used to produce infrared radiation from 509-514 cm^{-1}. The beam was multipassed 18-22 times through a pulsed planar supersonic expansion of a mixture of H_2O and He using a Herriot cell and detected using a helium-cooled (Si:B) photoconductive detector (IR Labs). The supersonic expansion was produced by bubbling pure He gas, with a backing pressure of 1-2 atm through liquid D_2O (Cambridge Labs, 99.96% purity), and then expanding through a 101.6 mm long slit at a repetition rate of 35 Hz into a vacuum chamber maintained at ~200mTorr by a Roots blower (Edwards 4200) backed by two rotary pumps (E2M 275) [26]. Simultaneously, the fringe spacing of a vacuum-spaced etalon and an OCS reference gas spectra were detected with a liquid He cooled (Cu:Ge) detector (Santa Barbara Research Center) and recorded to enable precise frequency calibration. The observed linewidths of ~ 30-40 MHz full-width half maximum (FWHM) are somewhat larger than the Doppler-limited linewidths extrapolated from earlier experiments using argon expansions. Typical frequency measurement accuracy is 10-20 MHz, limited by both linewidths of the cluster absorptions and laser drift. Spectra were detected in direct absorption using a time-gated phase sensitive signal processing approach.

Accessing the 500 cm^{-1} region of the electromagnetic spectrum has generally been notoriously difficult. The spectra reported here required the use of 10 separate laser diodes, each scanned across several modes to cover the specified spectral range. Moreover, large laser gaps are present in the spectra, which causes considerable difficulty in the assignment. Additionally, the spectrum reflects several distinct laser intensity fluctuations across different devices that are apparent in the complete spectra shown in Figure 2. Specifically, between 512.4 cm^{-1} and 513.2 cm^{-1} the intensity is enhanced and between 509.5 cm^{-1} and 510 cm^{-1} the intensity is depressed.

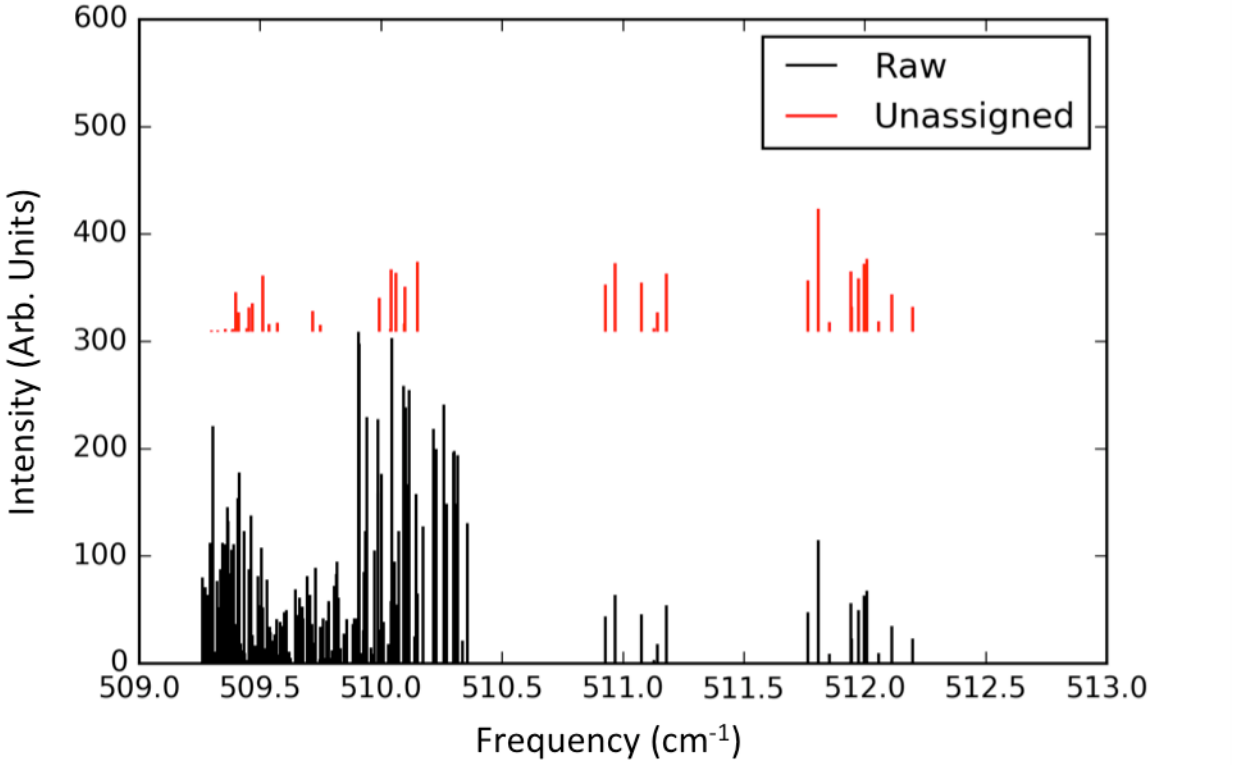

Figure 2: All transitions observed in the experimental range shown in black. Remaining unassigned transitions are shown in red.

Results and Analysis

Assignment

We have assigned 119 of the 188 observed transitions in the studied region. The transitions belong to three distinct parallel ($\Delta K = 0$) subbands, which are assigned to different tunneling levels of the water hexamer-d_{12} prism isomer. The observed transitions were fit to a near-prolate, rigid rotor model. This model is preferred to the asymmetric model due to the relatively small number of transitions observed which does not allow a fit without correlation. The equation for the fit is shown in equation 1.

Of course, since the transition assigned have a $\Delta K = 0$ we cannot separate the terms which only have K dependence; we will call this inseparable term, ΔM. The fit constants for the three subbands are shown in Table 1. Correlations matrices of the fit and a list of all assigned transitions are given in the supplementary information of this article.

Table 1: Fit constants for the near-prolate rigid rotor fit. All values are given in cm^{-1}, the uncertainty in the final digit for each constant is given in parenthesis. Primed values

correspond to excited state values, and double primed values are ground state constants.

	Subband 1	Subband 2	Subband 3
v	509.6317(69)	509.7526(42)	509.8594(61)
B'	0.03995(95)	0.03980(61)	0.03992(83)
ΔM	0.00503(12)	0.00513(64)	0.00495(90)
D_J'	-5.4(12)E-8	-1.2(98)E-6	-1.6(7.3)E-7
D_{JK}'	-3.9(4.7)E-6	-3.1(3.5)E-6	-3.8(7.7)E-6
B"	0.03914(94)	0.03902(68)	0.03909(77)
$D_J"$	1.7(1.2)E-7	-1.5(1.1)E-6	-9.7(7.7)E-7
$D_{JK}"$	-7.0(6.9)E-6	-5.1(3.5)E-6	-6.3(5.0)E-6

RMS	0.00134	0.00100	0.00111
Number of Transitions	37	45	37

Fit Analysis

We find a good quality of fit from the small number of observed transitions; the average RMS of the fit is ~33 MHz is a result of the wavelength accuracy of 10-20 MHz and the observed linewidths of 30-40 MHz. From the close agreement of all three subband's B" and B' values, we

conclude that these transitions originate from the same ground state and terminate in the same excited state. Additionally the B" value are in excellent agreement with the calculated absolute vibrational ground state value of 1167.6 MHz. As stated previously, the constant ΔM includes contributions from rotational constants A and B in addition to the centrifugal distortion constant D_K, unfortunately that makes it very difficult to obtain a value for the ΔA term which is essential to characterizing the vibrational mode. The most simplistic approach is to assume the contribution from D_K is negligible; then ΔM is equal to (ΔA - ΔB). Thus we can extract an average value for ΔA of 175.1 MHz.

Additionally, we can compare the centrifugal distortion constants to those observed previously for the $(H_2O)_6$ prism studied by Pérez et al [11]. In comparison, our values are typically an order of magnitude larger which could be a result of the heavy hydrogen isotopologue studied here. There is also a contribution from the relatively larger linewidths (30-40 MHz) which also leads to larger errors in the fit constants, similar to the fit results we have observed for the dimer, trimer, and pentamer in this region.

Tunneling Dynamics

We refer the reader to the recent work of Richardson et al for detailed treatment of the water hexamer prism's tunneling dynamics, and instead focus only of the relevant considerations made when studied the deuterated cluster [12]. Briefly, the prism hexamer's feasible tunneling motions can be described by the complete nuclear permutation inversion (CNPI) group isomoprphic to point group D_{2d}.

Previous work has shown that the water hexamer prism consists of two feasible tunneling motions (here we define 'feasible' as experimentally observed), which are referred to as P_a and P_g. In CNPI representation, P_a=(A D)(B F)(C E)(1 7)(2 8)(3 11)(4 12)(5 9)(6 10) where the labels correspond to the structure in Figure 1. The motion associated with this element is a double flip of the free hydrogens resulting in breaking one hydrogen bond. Likewise in CNPI notation, P_g=(A D)(B F)(C E)(1 8 2 7)(3 11)(4 12)(5 9)(6 10) and the motion is described as a double flip accompanied by a bifurcation and breaks two hydrogen bonds. The character table for this group is given in Table 2.

Table 2: Character table for the point group D_{2d}, group elements correspond to CNPI operations.

D_{2d}	E	$2P_g$	(12)(78)	$2P_a$	2(12)
A_1	1	1	1	1	1
A_2	1	1	1	-1	-1
B_1	1	-1	1	1	-1

B_2	1	-1	1	-1	1
E	2	0	-2	0	0
Γ_{ns}	531441	243	59049	729	177147
Γ_{dip}	3	-1	3	-1	3

The character representation of the nuclear spin wavefunction (Γ_{ns}) and the electric dipole moment (Γ_{dip}) are given at the bottom of Table 2. We can reduce Γ_{ns} to its irreducible representation:. For the fully deuterated hexamer prism the total spin wavefunction must transform as A_1 which leads to the spin statistical weights of A_1:A_2:B_1:B_2:E of 487:121:122:485:486. The irreducible representation of the electric dipole moment is and for parallel type ($\Delta K=0$) transitions the dipole transforms as B_2. Thus the expected selection rules are A_1 <-> B_2, A_2 <-> B_1, and E <-> E. These selection rules lead to a doublet of triplets pattern with a central doublet as shown in Figure 3. As shown by Richardson et al the energy level pattern of the hexamer prism is represented by the eigenvalue of the tunneling matrix shown in Figure 3A.

A) Tunneling Hamiltonian

$$\hat{H}=\begin{vmatrix} v & h_g & 0 & h_g & h_a & 0 & 0 & 0 \\ h_g & v & h_g & 0 & 0 & h_a & 0 & 0 \\ 0 & h_g & v & h_g & 0 & 0 & h_a & 0 \\ h_g & 0 & h_g & v & 0 & 0 & 0 & h_a \\ h_a & 0 & 0 & 0 & v & h_g & 0 & h_g \\ 0 & h_a & 0 & 0 & h_g & v & h_g & 0 \\ 0 & 0 & h_a & 0 & 0 & h_g & v & h_g \\ 0 & 0 & 0 & h_a & h_g & 0 & h_g & v \end{vmatrix}$$

B) Energy Level Diagram

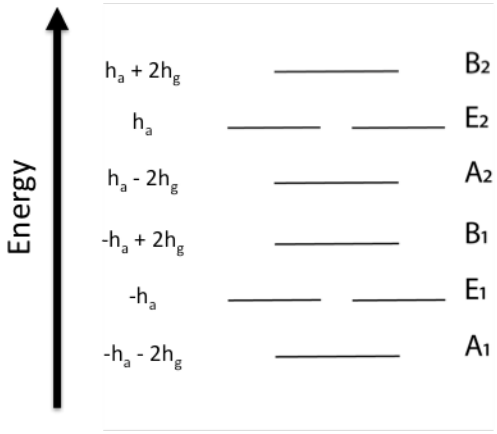

C) Transitions Energy Levels

$B_2 \rightarrow A_1 : E(J,K) - h_a' - h_a'' - 2h_g' - 2h_g''$

$E_2 \rightarrow E_1 : E(J,K) - h_a' - h_a''$

$A_2 \rightarrow B_1 : E(J,K) - h_a' - h_a'' + 2h_g' + 2h_g''$

$E_2 \rightarrow E_2 : E(J,K) + h_a' - h_a''$

$E_1 \rightarrow E_1 : E(J,K) - h_a' + h_a''$

$B_1 \rightarrow A_1 : E(J,K) + h_a' + h_a'' - 2h_g' - 2h_g''$

$E_1 \rightarrow E_2 : E(J,K) + h_a' + h_a''$

$A_1 \rightarrow B_2 : E(J,K) + h_a' + h_a'' + 2h_g' + 2h_g''$

D) Transition Energy Diagram

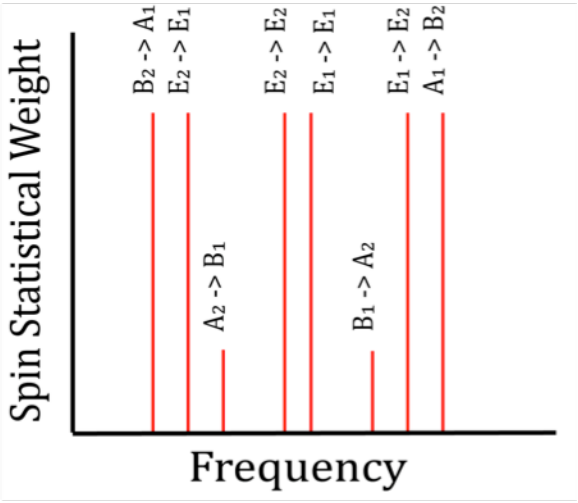

Figure 3: A) Tunneling Hamiltonian of the water hexamer prism. The term v represents the band origin. The terms h_g and h_a represent the tunneling splittings associated with group elements P_g and P_a respectively. B) Energy level diagram resulting from the two feasible tunneling motions present in the water prism hexamer. As a note, the subscript on the E symmetry labels merely corresponds to whether the level belongs to the upper (2) or lower (1) triplet. C) Energies of the selection rule allowed tunneling transitions for the prism hexamer. E(J,K) represents the typical near prolate, rigid rotor energy level. As a note the E_1 and E_2 energy levels refer to whether the level belongs to the upper or lower energy triplet C) Energy level diagram pictorially showing the energy level ordering shown in part B of this figure. The diagram assumes all tunneling elements are positive and $h_g' < h_g''$ which was an arbitrary choice for the figure.

Based on these considerations we tentatively assign the B_1 -> A_2, E_1 -> E_2, and A_1 -> B_2 transitions to subband 1, 2, and 3 respectively. This assignment is based on the equal spacing between three subbands and the intensity ratio of 1 : 1.1 : 1.3. While this intensity ratio doe not agree quantitatively with the expected ratio (based on spin statistics above), taking into consideration the large intensity fluctuations of the laser used, we consider this assignment as the most likely of those possible under parallel selection rules. Based on this assignment we can make an estimation of the tunneling element, h_g. The separation between subband 1 and subband 2 corresponds to the quantity $2h_g^{'}+2h_g^{"}$ where the prime and double prime represent the value in the excited and ground state respectively. The separation between subband 2 and 3 corresponds to the same quantity. From the measured values in the ground state (which are <1 MHz) we can explicitly calculate the value in the excited state (assuming these transitions originate in the ground vibrational state). Based on our fit values of the band origins, we find the average value of $h_g^{'}$ to be ~3400 MHz, which corresponds to a roughly 1000x enhancement of that tunneling splitting with respect the value in the ground state. This enhancement would be in keeping with the enhancement of tunneling splitting in the librational region observed for the water dimer, trimer, and pentamer.

Unassigned Transitions

Of the remaining 69 transitions observed, we have a partial assignment for 20 which belong to a parallel type transition with a band origin of 509.514 cm^{-1}. Due to the low number of transitions, a good quality fit could not be accomplished. However, this band may belong to the lower energy triplet predicted in Figure 3C specifically the A_2 -> B_1 transition. Indeed by fixing the lower state constants to the average we obtained here for our subband, the upper state constants for the fourth subband show good agreement with those of Table 1. We present the transitions assigned to this fourth subband in the SI of this article

Discussion

Vibrational Origin

As discussed above, the fit constants for the lower energy state show good agreement with the calculated value of B for the ground state. The theoretical value of 0.038949 cm^{-1} is in good agreement with the average of the three subbands observe here of 0.03909 cm^{-1}. We also note that these experiments are conducted in a supersonic expansion, which cools the rotational temperature to approximately 10 K, and the vibrational temperature to around 100K. **Theory goes here.** The most likely vibrational origin of the transitions is the ground state.

The nature of the excited state is harder to characterize, but the band origin of roughly 510 cm^{-1} indicates that the state lies in the librational region. We have previously investigated the water dimer, trimer, and pentamer in this spectral region and have found for all studied cluster anomalous behavior in context to lower frequencies [19-22]. Specifically we have observed large perturbations to the rigid rotor structure; observed as dramatic increases in centrifugal distortion constants. In this study we have observed an identical effect. Additionally,

while the ΔM term in the fit includes contributions from the D_K centrifugal distortion term, that contribution cannot fully account for what must be a extremely large change in the A rotational constant. Such a large magnitude change indicates dramatic vibrational motion along the A – axis of the molecule (which goes through the centers of the two trimer rings).

Librational Enhancement of Tunneling

As mentioned, we have previously studied the water dimer, trimer, and pentamer in the librational region and the most surprising observation has been the dramatic enhancement of the tunneling motions of these clusters. We observe a similar effect here, however we can only determine the enhancement of the h_g pathway. As described by Richardson et al, the h_g pathway's motions is characterized by a double flip accompanied by a bifurcation (**a figure of this would be nice**). The motion observed here involves breaking two hydrogen bonds whereas the previous studies involve breaking a single hydrogen bond. It would stand to reason that the previously observed enhancement would then not be observed; in contrast, we observe a 1000x enhancement relative to the observed ground state tunneling for the $(H_2O)_6$ prism. Due to larger mass weighted path for the $(D_2O)_6$ isotopologue we can expect the ground state tunneling for the heavier cluster to be smaller, thus the enhancement observed here larger.

This result is significant as the water hexamer represents a transition of minimum energy structure of water clusters from ring-like to a fully 3-D structure. The behavior of the water prism's tunneling motion has been predicted to possibly describe the motions of water in interfacial and confined environments; and thus the results presented here indicate that excitation to librational vibrations has a significant impact on tunneling dynamics.

Due to the absence of the lower energy triplet (from Figure 3C) we cannot characterize the h_a tunneling pathway in this excited state. The absence of this triplet is most likely a result of the large laser gaps present in the experiment coupled with the fact that the observed transitions fall on near the edge of the laser's spectral coverage. We can postulate that the band origin of the E_2 à E_1 transition must lie below 509.3 cm^{-1} (roughly the edge of spectral coverage), and thus the difference between that transition and the observed E_1 à E_2 transition would be at least 0.2 cm^{-1} which corresponds to an enhancement of nearly 6000x relative to the grounds state value for the $(H_2O)_6$ prism. This value is purely speculative based on the range of this experiment, and should not be taken as an absolute.

Conclusion

In summary, we have measured 3 parallel subbands belonging to a common librational excitation for the $(D_2O)_6$ prism cluster. Assigning the transitions to tunneling sublevels allows us to extract a value of ~3400 MHz for the h_g tunneling motion representing a nearly 1000x enhancement of the pathway relative to the ground state observed for the $(H_2O)_6$ cluster. This enhancement is in keeping with the dramatic enhancement observed previously for the water dimer, trimer, and pentamer in the same experimental region.

From comparison to theoretical calculations, we find the observed change in the B rotational constant to be consistent; however the observed change in the A rotational constant (approximated here as ΔM) is dramatically larger than prediction. This large change indicates a

large increase in motion along the A-axis of the molecule and give some clue as to the nature of the vibrational motion. Further study is warranted to investigate this excited state.

Supplemental Information

The supplemental information of this article contains a list of all assigned transitions in Table S1, and correlation matrices for the fits in Table S2.

Acknowledgments

RICH need your help here; do we still need to cite NSF?
The authors acknowledge funding from CALSOLV an affiliate program of RESOLV (Ruhr-Unversitaet Bochum).

References

1. Clary, D.C., *Quantum Dynamics in the Smallest Water Droplet.* Science, 2016. **351**(6279).
2. Keutsch, F.N. and R.J. Saykally, *Water Clusters: Untangling the Mysteries of the Liquid, One Molecule at a Time.* PNAS, 2001. **98**(19).
3. Mukhopadhyay, A., W.T.S. Cole, and R.J. Saykally, *The water dimer I: Experimental characterization.* Chemical Physics Letters, 2015. **633**: p. 13-26.
4. Babin, V. and F. Paesani, *The curious case of the water hexamer: Cage vs. Prism.* Chemical Physics Letters, 2013. **580**: p. 1-8.
5. Paesani, F., *Getting the Right Answers for the Right Reasons: Toward Predictive Molecular Simulations of Water with Many-Body Potential Energy Functions.* Acc Chem Res, 2016. **49**(9): p. 1844-51.
6. Brown, S.E., et al., *Monitoring Water Clusters "Melt" Through Vibrational Spectroscopy.* J Am Chem Soc, 2017. **139**(20): p. 7082-7088.
7. Huang, Y., et al., *Hydrogen-bond relaxation dynamics: Resolving mysteries of water ice.* Coordination Chemistry Reviews, 2015. **285**: p. 109-165.
8. Liu, K., et al., *Characterization of a Cage Form of the Water Hexamer.* Nature, 1996. **381**.
9. Pham, C.H., et al., *Many-Body Interactions in Ice.* J Chem Theory Comput, 2017. **13**(4): p. 1778-1784.
10. Liu, K., M.G. Brown, and R.J. Saykally, *Terahertz Laser Vibration−Rotation Tunneling Spectroscopy and Dipole Moment of a Cage Form of the Water Hexamer.* The Journal of Physical Chemistry A, 1997. **101**(48): p. 8995-9010.
11. Perez, C., et al., *Structures of cage, prism, and book isomers of water hexamer from broadband rotational spectroscopy.* Science, 2012. **336**(6083): p. 897-901.

12. Richardson, J.O., et al., *Concerted Hydrogen-Bond Breaking by Quantum Tunneling in the Water Hexamer Prism.* Science, 2016. **351**(6279).
13. Bates, D.M. and G.S. Tschumper, *CCSD(T) Complete Basis Set Limit Relative Energies for Low-Lying Water Hexamer Structures.* J. Phys. Chem. A, 2009. **113**.
14. Head-Gordon, M. and T. Head-Gordon, *Analytic MP2 Frequencies without fifth-order storage. Theory and application to bifurcated hydrogen bonds in the water hexamer.* Chem. Phys. Lett., 1994. **220**.
15. Kim, J. and K.S. Kim, *Structures, binding energies, and spectra of isoenergetic water hexamer clusters: Extensive ab initio studies.* The Journal of Chemical Physics, 1998. **109**(14): p. 5886-5895.
16. Kim, K., K.D. Jordan, and T.S. Zwier, *Low-Energy Structures and Vibrational Frequencies of the Water Hexamer: Comparison with Benzene-(H2O)6.* J. Am. Chem. Soc., 1994. **116**.
17. Wang, Y., et al., *The water hexamer: cage, prism, or both. Full dimensional quantum simulations say both.* J Am Chem Soc, 2012. **134**(27): p. 11116-9.
18. Perez, C., et al., *Hydrogen bond cooperativity and the three-dimensional structures of water nonamers and decamers.* Angew Chem Int Ed Engl, 2014. **53**(52): p. 14368-72.
19. Cole, W.T.S., et al., *Far-infrared VRT spectroscopy of the water dimer: Characterization of the 20 mum out-of-plane librational vibration.* J Chem Phys, 2015. **143**(15): p. 154306.
20. Cole, W.T.S., et al., *Hydrogen bond breaking dynamics in the water pentamer: Terahertz VRT spectroscopy of a 20 mum libration.* J Chem Phys, 2017. **146**(1): p. 014306.
21. Keutsch, F.N., et al., *Hydrogen Bond Breaking Dynamics of the Water Trimer in the Translational and Librational Band Region of Liquid Water.* J. Am. Chem. Soc., 2001. **123**.
22. Keutsch, F.N., et al., *Far-infrared laser vibration–rotation–tunneling spectroscopy of water clusters in the librational band region of liquid water.* The Journal of Chemical Physics, 2001. **114**(9): p. 4005-4015.
23. Cole, W.T.S., et al., *Far-infrared VRT spectroscopy of the water dimer: Characterization of the 20 um out-of-plane librational vibration.* J Chem Phys, 2015. **143**(15): p. 154306.
24. Blake, G.A., et al., *Tunable Far Infrared Laser Spectrometers.* Rev. Sci. Instrum., 1991. **62**(7).
25. Blake, G.A., et al., *The Berkeley Tunable Far Infrared Laser Spectrometers.* Rev. Sci. Instrum., 1991. **62**(7).
26. Liu, K., et al., *A long path length pulsed slit valve appropriate for high temperature operation: Infrared spectroscopy of jet-cooled large water clusters and nucleotide bases.* Review of Scientific Instruments, 1996. **67**(2): p. 410-416.